JPE 9-6-10

Sensorless Control of a Single-Phase Switched Reluctance Motor Using Residual Flux

Hyong-Yeol Yang†, Duck-Shick Shin*, and Young-Cheol Lim**

†Dept. of Electrical Eng., Honam University, Gwangju, Korea
*Dept. of Digital Convergence Research Center, Korea Electronics Technology Institute, Gwangju, Korea
**Dept. of Electrical Eng., Chonnam National University, Gwangju, Korea

ABSTRACT

This paper presents a new sensorless control method for single-phase switched reluctance motors using induced electromotive force (EMF) due to the residual flux both on the stator and the rotor during phase commutation. The induced EMF falls to zero when the rotor pole moves away from the overlap with the stator pole. By detecting this instant, the speed and position of the rotor can be simply estimated. This method is very simple to implement and it is insensitive to variations in the system parameters as it does not require any stored magnetic data or offline inductance measurements but requires only measurements of the terminal voltage and a simple analog circuit. The proposed method is implemented on a 6/6 single-phase switched reluctance motor. However, it can also be implemented on a multiphase SRM regardless of the size, operation speed and switching mode of the motor hence making the proposed method viable to many applications. Simulation and experimental verification is provided to demonstrate the feasibility of the proposed method.

Keywords: Position estimation, Sensorless control, Switched reluctance motor, Residual flux

1. Introduction

Simple structure, low manufacturing costs, fault tolerance capability, along with a broad choice of both motor and converter topologies depending on the requirements of the application, have made the switched reluctance motor (SRM) a viable option for many applications such as aerospace, automotives, traction drives, automation, home appliances, etc. An SRM requires a shaft position transducer for its proper control. For low performance drives, the position sensors are often realized using Hall-effect-based sensors or opto-interrupters. For high performance drives, higher resolution can be obtained via resolvers or optical encoders. These sensors, however, add to the size and cost of the overall drive system and decrease system reliability [1].

Therefore, to avoid these negatives, various types of indirect position estimation and control methods eliminating the need for position sensors [2-7] have been proposed. Most sensorless techniques utilize the SRMs' unique relationship between flux linkage (or inductance),

Manuscript received May 7, 2009; revised Sept. 25, 2009
†Corresponding Author: sfish2000@gmail.com
Tel: +82-62-940-5077, Fax: +82-62-940-5072, Honam Univ.
Dept. of Electrical Eng., Honam Univ., Korea
*Dept. of Digital Convergence Research Center, Korea Electronics Technology Institute, Korea
**Dept. of Electrical Eng., Chonnam Nat'l Univ., Korea

rotor position and phase current. However, these approaches require accurate magnetization characteristics of the motor, often involving off-line measurements and/or complex computations [2-6]. The approach proposed in [7] is simple to implement in that the controller detects the rotor position where a rotor pole and a stator pole begin to overlap by monitoring the rate of change in the current by using an analog circuit. However, this approach necessitates phase excitation with an advance angle. A method using search coils [8] estimates the rotor position by detecting the change of the back-EMF but it also requires an advancing of the turn-on angle. Additional manufacturing costs and effort are the major drawback of this method.

This paper proposes a simple method to estimate rotor position utilizing the effect of the residual flux that remains in the stator and rotor poles during commutation. In normal motoring operation, the power switches of the converter should be turned off in such a way as to achieve fast commutation and hence to avoid significant negative torque generation. When the switches are turned off, a negative voltage across the winding, i.e., -Vs, is applied while the current flows back to the dc link through the freewheeling diodes. However, even after the current decays to zero, a small negative voltage still remains across the winding terminal. This is because a small EMF is induced due to the residual flux in the stator and rotor poles while the rotor is rotating. Thus, the terminal voltage falls to zero when the rotor pole is completely out of overlap with the stator pole. By detecting this instant and setting the position at this instant as an index position, the angular position and speed of the rotor can be simply estimated. The proposed approach is very simple to implement as it only requires measurement of the terminal voltage with a simple analog detection circuit. The proposed method is demonstrated via simulation and experimental tests.

2. Rotor Position Estimation

2.1 Basic Theory

Fig. 1 shows the configuration of a single-phase 6/6 SRM in conjunction with the asymmetric bridge converter employed in the presented study. The six individual

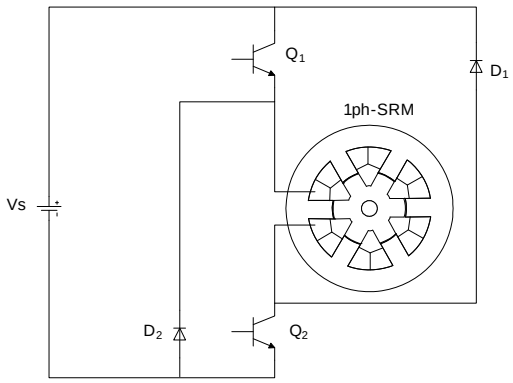

Fig. 1. Single-phase SRM drive.

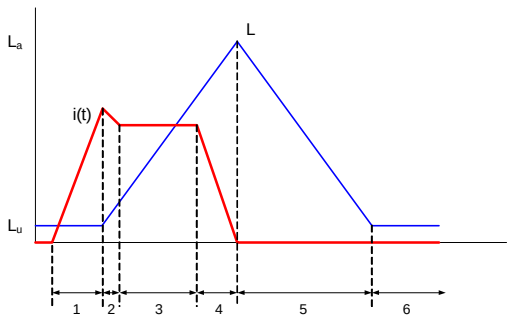

Fig. 2. Phase current and inductance profile with respect to the rotor position.

windings of each stator pole are connected in series to form a single-phase stator winding.

The voltage equation of the SRM is given by:

$$v = Ri + \frac{d\lambda(\theta, i)}{dt} = Ri + L\frac{di}{dt} + i\frac{\partial L}{\partial \theta}\omega \quad (1)$$

where R, $\lambda(\theta,i)$, and L denote the winding resistance, flux linkage and inductance, respectively.

Neglecting magnetic saturation and nonlinearity, the voltage equation for each region within an excitation cycle as shown in Fig. 2 can be expressed as follows:

$$\text{Region 1: } v = Ri + L\frac{di}{dt} \quad (2)$$

$$\text{Region 2: } v = Ri + L\frac{di}{dt} + i\frac{\partial L}{\partial \theta}\omega \quad (3)$$

Region 3: $v = Ri + i\frac{\partial L}{\partial \theta}\omega$ (4)

Region 4: $v = Ri + L\frac{di}{dt} + i\frac{\partial L}{\partial \theta}\omega$ (5)

Region 5: $v = Ri + i\frac{\partial L}{\partial \theta}\omega = 0 \ (\because i = 0, \frac{di}{dt} = 0)$ (6)

Region 6: $v = Ri = 0 \ (\because i = 0, \frac{di}{dt} = \frac{\partial L}{\partial \theta} = 0)$ (7)

Ideally, in regions 5 and 6, the phase current falls to zero and hence the voltage across the winding is zero. However, in practice, a small negative voltage still remains across the winding due to a small induced EMF that results from residual flux in the stator and rotor poles. The flux linkage, λ_r due to this residual flux leads to an induced EMF by Faraday's law of induction:

$$v = -\frac{d\lambda_r}{dt} = -\frac{d\lambda_r}{d\theta}\omega \quad (8)$$

This induced EMF is proportional to the rate of change in the flux and the rotor speed. Assuming the motor is running at a constant speed, the induced EMF is proportional to the rate of change of λ_r with respect to the rotor position and this will in turn yield information on the rotor's position.

If there is no current flowing through the winding, the residual flux and its rate of change with respect to the rotor position is shown in Fig. 3. From Fig. 3, it can be seen that the induced EMF falls to zero at the unaligned position (52°) where the stator and rotor poles become out of overlap. Since the phase current is zero, this unaligned position can be detected regardless of the level of phase current. By using the detected unaligned position as an index position, the rotor speed and position can be estimated for sensorless operation of the considered single-phase SRM.

2.2 Induced EMF Due to Residual Flux without Excitation

In order to investigate the induced EMF due to the effect of residual flux, a simulation using Maxwell 2D

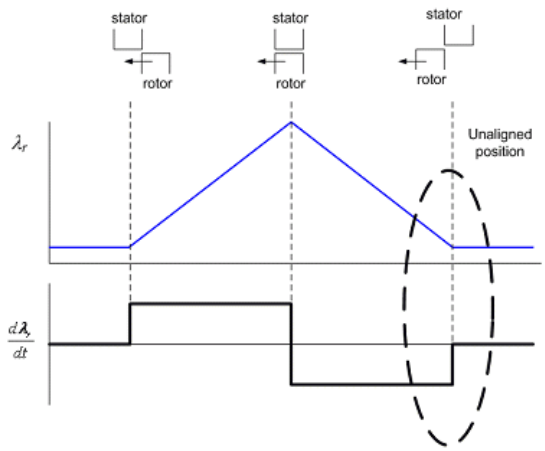

Fig. 3. Residual flux linkage and its rate of change with respect to the rotor position.

software is conducted as follows. After the motor has been running in normal operation for some time, excitation is terminated but the motor is forced to run at 600rpm by an external source without the motor being excited. The residual flux in the stator and rotor pole results in a small voltage induced across the winding terminal. Fig. 4(a) and (b) show the residual flux linkage and the induced EMF from the winding terminal, respectively. It can be seen that the flux linkage and the induced EMF fluctuate periodically with an alternating amplitude, i.e., ±600mV and ±400mV. This is because the rotor poles experience a flux reversal every alternate cycle. Fig. 4(c) shows the flux paths of a single-phase SRM with six stator poles and six rotor poles with respect to the rotor position. The direction of the rotor flux opposes that of the stator every alternate cycle in a fashion that leads to a partial addition or a cancellation of the overall flux. Fig. 6 shows the measured terminal voltage which correlates well with the simulation results.

2.3 Effect of Induced EMF of the Motor at Steady-state

Fig. 6 shows simulated waveforms of the flux linkage and the voltage across the stator winding when the motor is running at 1800rpm. The voltage across the winding becomes negative after the switch is turned off and reaches zero when the winding current falls to zero.

However, due to the residual flux in the rotor pole, a

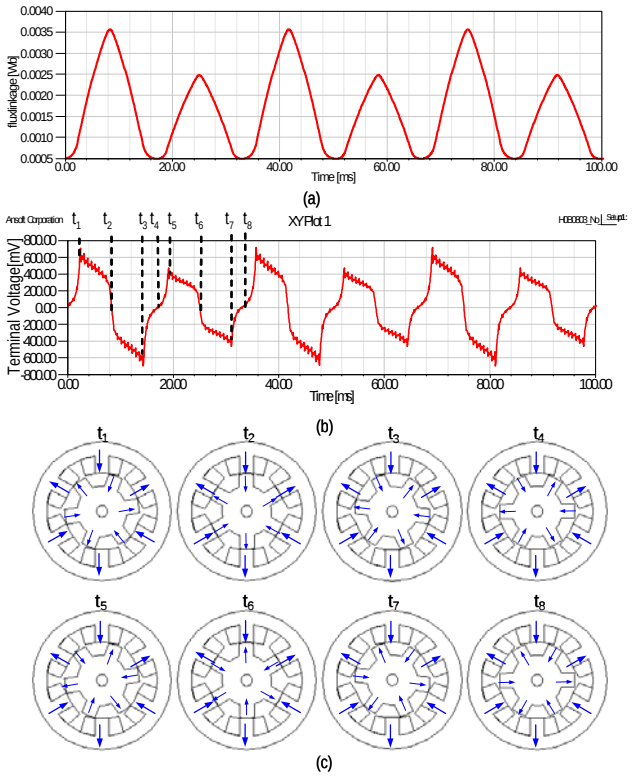

Fig. 4. (a) Flux linkage (the motor is running at 600 rpm), (b) Terminal voltage (the motor is running at 600 rpm) and (c) Flux paths of a 6/6 single-phase SRM with respect to the rotor position.

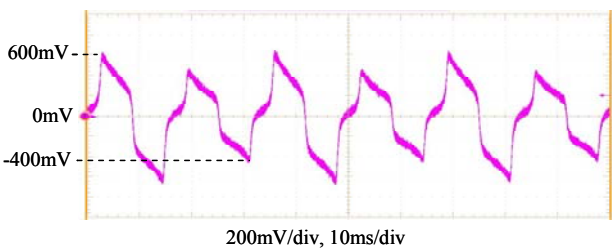

Fig. 5. Measured terminal voltage without excitation (the motor is running at 600 rpm).

negative non-zero voltage across the winding remains for a while until the rotor pole moves away from the overlap with the stator pole completely. Hence, by monitoring this absolute position, where the induced voltage becomes zero can be determined.

2.4 Detection of Unaligned Position

The measured terminal voltage is processed to generate

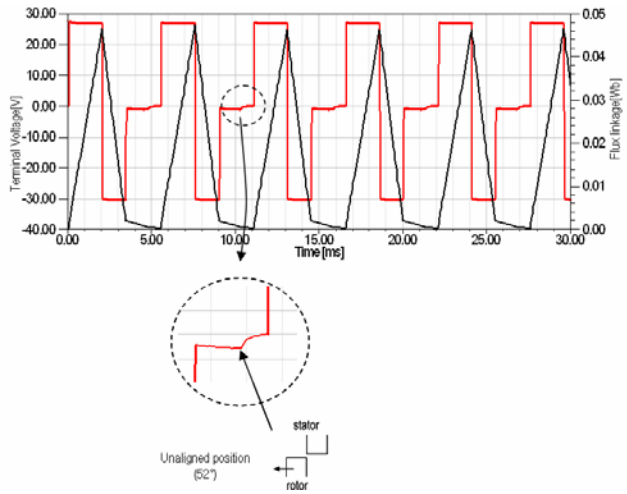

Fig. 6. Flux linkage and terminal voltage (motor running at 1800 rpm).

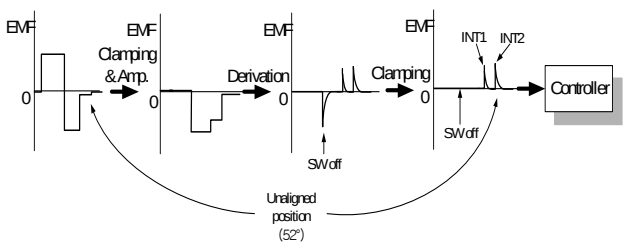

Fig. 7. Detection of the unaligned position.

interrupt signals for detection of the unaligned position as depicted in Fig.7. Since the induced EMF is small at low speeds, the measured voltage is amplified so as to facilitate position detection in low speed operation. As shown in Fig. 7, the positive voltage is clamped and hence only the negative value is amplified. Then, differentiation of the amplified signal results in one negative and two positive pulses. After the negative pulse is clamped, the second one among the two positive pulses is used as an interrupt signal to the DSP controller, indicating the position where the rotor pole moves away from the overlap with the stator pole, i.e., 52°.

3. Estimation of Rotor Speed and Position

By measuring the time interval between two consecutive unaligned positions, i.e. two consecutive INT2 signals, the rotor speed can be calculated. This can be easily accomplished using a timer counter in the DSP

controller. Once the rotor speed is determined, the rotor position can be calculated as follows.

In the considered 6/6 single-phase SRM, the commutation period is 60°. Therefore, the unaligned position is detected every 60°, i.e., six times per revolution. The speed is calculated as:

$$\omega = \frac{d\theta}{dt} = \frac{60°}{\Delta t} \times \frac{\pi}{180°} [rad/s] \tag{9}$$

where Δt is the time it takes for the rotor to rotate 60°, as measured by a timer. The rotor position is calculated as:

$$\theta = 52° + \left(60° \times \frac{N_t}{N_p} \right) \tag{10}$$

where N_t is the number of the timer count between the unaligned position (52°) and the current position and N_p is the number of the timer count for a 60° rotation. The timer is reset to zero when the unaligned position is detected and hence θ is bounded between 0 to 59°. The turn-on and turn-off angles are determined based on the estimated rotor position.

4. Starting Algorithm

A single-phase motor with six stator poles and six rotor poles is employed in the experimental drive system. The motor has a parking magnet attached to the stator pole for reliable starting so that at standstill the rotor is located in a position where the rotor pole is overlapped with the stator pole (8°) and hence is capable of generating starting torque. The starting scheme depicted in Fig. 8 is described as follows. When the switch is turned on, the motor starts rotating. In about 9ms, when the rotor is located at 23°, the switch is turned off. The time for the rotor to move from 8° to 23° is dependent on the required starting torque and it is determined by a few trial and error tests from a position sensor based system. However, the exact time is not necessary for successful starting.

When the switch is turned on, the current flows through the winding and hence magnetizes the motor. Once the motor is magnetized, some residual flux still remains in the iron of the stator and rotor poles even after the switch is turned off. By monitoring the change in the terminal voltage due to the residual flux when the rotor moves away from the overlap with the stator, the first detection of the unaligned position can be obtained as can consecutive detections. That way, successful starting of the motor is achieved.

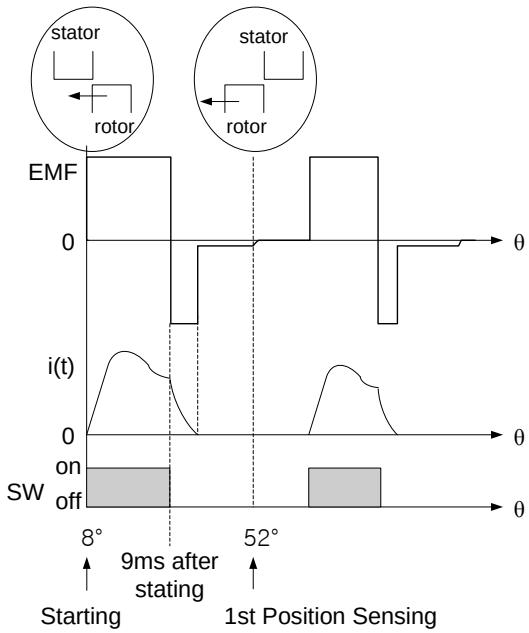

Fig. 8. Sensorless starting.

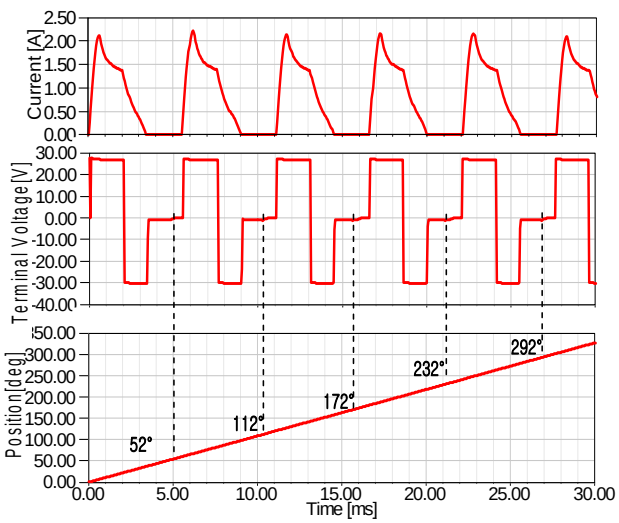

Fig. 9. Simulation results (Current, terminal voltage, rotor position).

5. Simulation and Experimental Results

The proposed sensorless scheme is verified by simulation and experimental tests and they are described in this section. Fig. 9 shows the simulation results obtained from Maxwell 2D software. The current, voltage, and rotor position are plotted. It can be seen that the rotor position where the terminal voltage falls to zero corresponds to each unaligned position (52°, 112°, 172°, 232° and 292°) within one revolution.

Fig. 10 shows the experimental single-phase SRM with a fan attached to the shaft as a load. The specifications of the motor are summarized in Table 1. Fig. 11 depicts a block diagram of the proposed sensorless drive system. As shown in Fig. 11, the rotor position where the terminal voltage falls to zero is detected by the analog detection circuit and the generated detection signal is fed to the external interrupt terminal of the DSP controller for estimation of rotor speed and position.

Table 1. Specification of the single-phase SRM.

Parameter		Value
Stator	Outer diameter(mm)	100
	Inner diameter(mm)	54.6
	Yoke Thickness(mm)	10
	Number of Pole	6
	Pole angle(deg)	22
Rotor	Outer diameter(mm)	54
	Inner diameter(mm)	8
	Yoke Thickness(mm)	14
	Number of Pole	6
	Pole angle(deg)	22
Number of winding for a pole(turns)		70
Stack length(mm)		34
Air gap(mm)		0.3

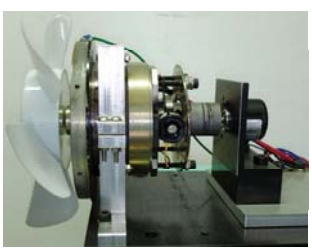

Fig. 10. Experimental setup for the single-phase SRM.

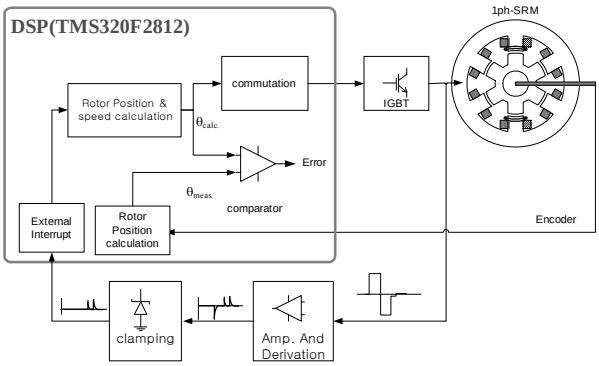

Fig. 11. Block diagram of the proposed sensorless single-phase SRM drive.

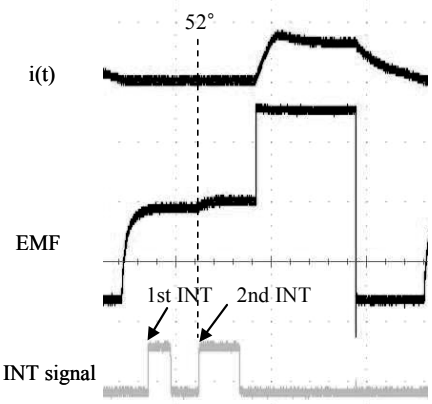

Fig. 12. Experimental results: Measured current, terminal voltage, and interrupt signals.

Fig. 12 shows the measured waveforms of the current, the terminal voltage and the interrupt signal generated by the change in terminal voltage when the motor is running with the position feedback from an encoder. The test is only to verify the performance of the detection circuit such that the interrupt signal is generated from the change of the induced EMF.

A comparison between sensor-based and sensorless operation is shown in Fig. 13. It is observed that the maximum deviation between the actual and estimated rotor position is less than 1 degree when the motor is running at 2000rpm. From Fig. 13, it can be seen that the proposed sensorless scheme is comparable to sensor-based operation. Additional experiments for sensorless operation with different advance angles are shown in Fig. 14.

Another experimental result is shown in Fig. 15 to verify the feasibility of the proposed method in PWM

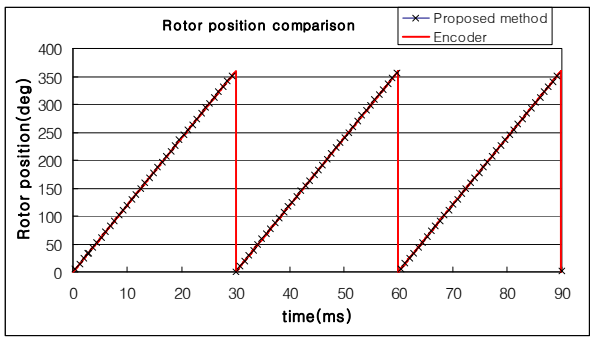

Fig. 13. Comparison of encoder-based operation and proposed sensorless operation at 2000rpm.

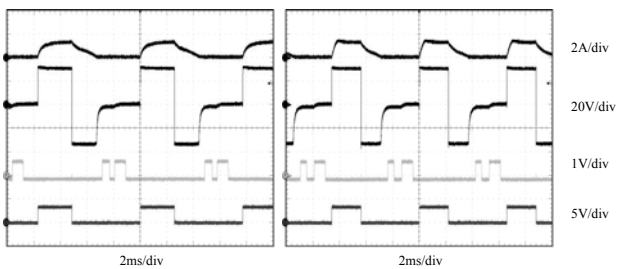

(a) (b)

Fig. 14. Experimental results for sensorless operation (Single-pulse operation). (a) Advanced angle = 0°, 1300rpm (b) Advanced angle = 3°, 1500rpm.

mode at 700rpm. Fig. 15 shows the measured waveforms for sensorless operation in PWM mode. The negative voltage applied during the excitation also generates interrupt signals. However, these signals do not affect the performance of the detection circuit as the interrupt signal is generated after the commutation starts is taken for position estimation.

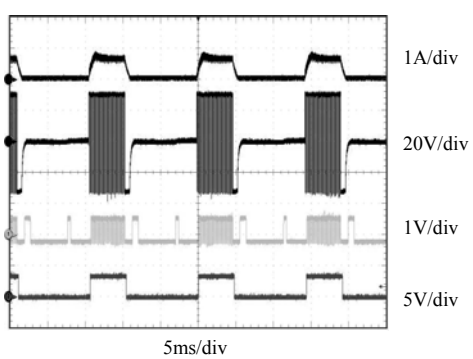

Fig. 15. Experimental results for sensorless operation in PWM operation.

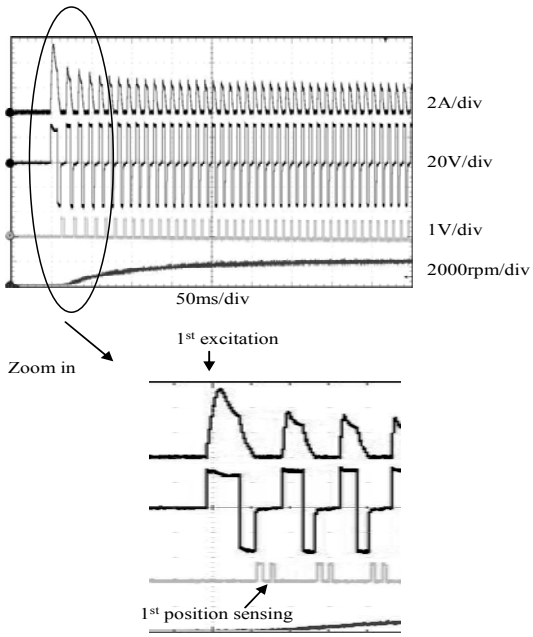

Fig. 16. Sensorless self-starting from standstill.

Fig. 16 shows the execution of sensorless starting. The motor starts from standstill and reaches the commanded speed. After the first open-loop excitation, the detection of the unaligned positions is executed successfully. Fig. 16 also shows the dynamic performance of the proposed method while the speed changes.

6. Conclusions

This paper proposes a new method of sensorless position estimation and control for a single-phase SRM. First, the effect of the residual flux is investigated by simulation. The proposed method is verified by simulation and experimental results. Sensorless operation with different advance angles as well as comparison with sensor-based operation has been conducted to demonstrate the feasibility of the proposed method.

The proposed sensorless scheme is very simple and robust to system parameter variation since it only requires measurement of the terminal voltage and a simple analog circuit without any pre-stored magnetic characteristics of the motor. This method can be implemented regardless of the size, operation speed, and switching mode of the motor, making the proposed method viable for many applications. Although the method is demonstrated on a single-phase, it

can also be implemented on a multiphase SRM.

References

[1] T.J.E. Miller, "Switched Reluctance Motors and Their Control," *Magna Physics Publishing and Clarendon Press*. 1993.

[2] J. W. Ahn and S. J. Park, "An Analog Encoder for Precise Angle Control of SRM," *Journal of Power Electronics*, KIPE, Vol. 3, No. 3, pp. 167-174, 2003.

[3] B. Fahimi, G. Suresh, and M. Ehsani, "Review of sensorless control methods in switched reluctance motor drives," Conf. Rec. of the 2000 IEEE Ind. Appl. Conf., Vol. 3, pp. 1850-1857, Oct. 2000.

[4] R. Krishnan, "Sensorless operation of SRM drives: R & D status," *The 27th Ann. Conf. of the IEEE Ind. Electr. Soc*., Vol. 2, pp. 1498-1503, Nov.-Dec. 2001.

[5] E. Mese, and D. A. Torrey, "An approach for sensorless position estimation for switched reluctance motors using artifical neural networks," *IEEE Trans. on Power Electr*., Vol. 17, Issue: 1, pp. 66-75, Jan. 2002.

[6] I.-W. Yang, and Y.-S. Kim, "Rotor speed and position sensorless control of a switched reluctance motor using the binary observer," *IEE Proc.-Electr. Power Appl*., Vol. 147, No. 3, pp. 220-226, 2000.

[7] G. Gallegos-Lopez, P. C. Kjaer, T. J. E.Miller, "A New Sensorless Method for Switched Reluctance Motor Drives," *IEEE Trans. on Industry Appl*., Vol. 34, No. 4, pp. 832-840, 1998.

[8] H. Y. Yang, J.G. Kim, Y.C. Lim, S. K. Jeong, and Y. G. Jung, "Position detection and drive of a toroidal Switched Reluctance Motor(TSRM) using searchcoils," *IEE Proc.-Electr. Power Appl*., Vol. 151, No. 4, pp. 377-384, July 2004.

Hyong-Yeol Yang was born in Chonnam, Korea in 1969. He received a B.S. degree in electrical engineering from Chonnam National University, Gwangju, Korea in 1993. He received a M.S. and Ph.D. in electrical engineering from Chonnam National University in 1998 and 2004 respectively. His research experience includes work done with Hyundai Motor Company, the Regional Research Center for High-quality Electric Component and Systems at Chonnam National University, Honam University and G-Auto Co., Korea. He has also done visiting research at Virginia Tech., USA. He is currently a full time lecturer in the department of Electrical Engineering at Honam University, Gwangju, Korea. His main research interests are in the areas of fuzzy logic control, design and drives of electric machines, and applications using microcontrollers.

Duck-Shick Shin was born in Chonnam, Korea, in 1979. He received a B.S. degree in electrical engineering from Honam University, Gwangju, Korea, in 2004 and, a M.S degree from Chonnam National University, Gwangju, Korea, in 2006. Since 2006, he has been with the Researcher in Digital Convergence Research Center at the Korea Electronics Technology Institute, Korea. His research interests included power electronics and motor control and design.

Young-Cheol Lim was born in Chonnam, Korea, in 1953. He received a B.S. degree in electrical engineering from Chonnam National University, Gwangju, Korea, in 1975, and a M.S and Ph.D. from Korea University, Seoul, Korea, in 1977 and 1990, respectively. Since 1981, he has been a Professor at Chonnam National University, where he was the Director of the Research Center for High-quality Electric Components and Systems from 1998 to 2007. His current research interests include power electronics, control instruments, and neuro-fuzzy control. He is the author or coauthor of three books and more than 200 published technical papers. Prof. Lim has been a member in various academic societies such as the Korean Institute of Power Electronics (KIPE), the Korean Institute of Electrical Engineers (KIEE) and the Institute of Control, Automation and Systems Engineers, Korea. He has received a number of awards, including the 1997 KIEE Best Paper Award, the 1998 KIEE Meritorious Award, the 2000 KIPE Best Paper Award and the 2001 KIPE Academic Award.